Journal of Inorganic Biochemistry 166 (2017) 55–63

Contents lists available at ScienceDirect

Journal of Inorganic Biochemistry

journal homepage: www.elsevier.com/locate/jinorgbio

Synthesis of Ag(I) camphor sulphonylimine complexes and assessment of their cytotoxic properties against *cisplatin*-resistant A2780cisR and A2780 cell lines

João M.S. Cardoso [a], Isabel Correia [a], Adelino M. Galvão [a], Fernanda Marques [b], M. Fernanda N.N. Carvalho [a,*]

[a] Centro de Química Estrutural, Instituto Superior Técnico, Universidade de Lisboa, Av. Rovisco Pais 1049-001, Lisboa, Portugal
[b] Centro de Ciências e Tecnologias Nucleares (C^2TN), Instituto Superior Técnico, Universidade de Lisboa, Estrada Nacional 10 (km 139,7), 2695-066 Bobadela LRS, Portugal

ARTICLE INFO

Article history:
Received 28 June 2016
Received in revised form 10 October 2016
Accepted 3 November 2016
Available online 4 November 2016

Keywords:
Silver complexes
Camphorsulphonylimines
Synthesis
Cytotoxic properties
DNA binding

ABSTRACT

Camphorsulphonylimine complexes $[Ag(NO_3)(^{I}L)_2]$ ($^{I}L = C_{12}H_{19}N_3SO_2$, **1**) and $[(AgNO_3)_2(^{II}L)]$ ($^{II}L = C_{22}H_{23}N_3SO_2$, **2**) were synthesized and characterized by elemental analysis, spectroscopy (IR, NMR) and cyclic voltammetry. $[Ag(NO_3)(^{I}L)_2]$ crystalizes in the monoclinic C2 space group with a triangular geometry assuming a chalice-type shape. The anti-proliferative properties of the new complexes **1** and **2** and those of the previously reported $[Ag(NO_3)(^{III}L)]$ ($^{III}L = C_{16}H_{18}N_3SO_2$, **3**) were assessed against the human ovarian cancer cells (*cisplatin*-sensitive A2780, *cisplatin*-resistant A2780cisR) and the non-tumoral human HEK 293 cell line, using the MTT [3-(4,5-dimethylthiazol-2-yl)-2,5-diphenyltetrazolium bromide] assay. The NR (3-amino-7-dimethylamino-2-methylphenazine hydrochloride) assay was alternatively used to assess the cytotoxicity on the A2780 cells. Results from the MTT assay (48 h exposure) show that the complexes display IC_{50} values lower (by at least one order of magnitude) than *cisplatin*, while the cytotoxicity of $AgNO_3$ is of the same order of *cisplatin*. The camphorsulphonylimine ligands display irrelevant (^{I}L, ^{III}L) or no cytotoxicity (^{II}L). The highest cytotoxicity (lower IC_{50}) was found for $[(AgNO_3)_2(^{II}L)]$. The binding ability of the complexes to calf thymus-deoxyribonucleic acid (CT-DNA) was studied by fluorescence. Constants (K_{sv}, K_a) and the number (n) of binding centres to DNA were calculated showing that DNA intercalation possibly occurs in the cases of complexes **2** and **3**, while a more complicated process operates for **1**. As expected from the cytotoxicity, $[(AgNO_3)_2(^{II}L)]$ displays the highest binding affinity ($K_a = 1.61 \times 105\ M^{-1}$). No binding to DNA was detected for $AgNO_3$ or ^{II}L under the experimental conditions used. The binding trend to CT-DNA found by fluorescence was corroborated by cyclic voltammetry.

1. Introduction

The battle against cancer is far from being won despite therapies based on natural and synthetic products, microorganisms or other strategies being essayed. Design and synthesis of new compounds with anticancer activity with low side effects and/or complementary antimicrobial properties remains a challenge to synthetic chemists. Decrease of the organism defenses with enhanced vulnerability to infection by microorganisms (bacteria or fungus) commonly accompanies cancer treatment, a fact that compounds with bactericide and or fungicide properties may help to overcome. A large pool of compounds with anti-proliferative activities against cancer-cells is thus desirable to provide pharmaceutical industries or eventually university start-ups with a wide variety of options to assess the possibility of clinical trials. Consequently, academic and industrial research on compounds with cytotoxic activity has to continue till efficiency reaches the goal of fighting and win the battle against several types of cancer.

Silver based compounds have not yet been much investigated as cytotoxic agents, although some of them (e.g. silver nitrate or silver sulfadiazine) have well recognized pharmacological properties [1–6] as antimicrobial agents. A slow increase in the number of publications dealing with the medicinal properties of silver complexes shows that several complexes have promising anticancer activities [7–13], particularly relevant against *cisplatin* resistant cell lines [14–16] as well as medicinal applications as nanoparticles or coating agents due to their antimicrobial properties. [17–20].

Another branch of long lasting pharmaceutical compounds whose cytotoxic properties [21] have been scarcely assessed is that of camphor derived compounds. In particular camphor derivatives of the imine ($OC_{10}H_{14}NY$) or sulphonylimine ($SO_2NC_{10}H_{13}NY$) types are quite attractive as ligands to coordinate transition metals and generate complexes sterically and electronic versatile due to a variety of available substituents (Y). There is evidence that camphor complexes display enhanced activity compared to free camphor ligands.[22] Silver nitrate was considered as a suitable precursor to synthesize camphor complexes, potentially active against the proliferation of cancer cells, based on a former study which showed that camphor Cu(I) complexes

* Corresponding author.
E-mail address: fcarvalho@ist.utl.pt (M.F.N.N. Carvalho).

http://dx.doi.org/10.1016/j.jinorgbio.2016.11.003
0162-0134/

have cytotoxic activity.[23] Encouraged by that study, this work aims at assessing the cytotoxic activity of camphorsulphonylimine Ag(I) complexes towards ovarian cancer cells A2780/A2780cisR (cisplatin sensitive and resistant cells) and compare the results with those displayed by cisplatin in the same experimental conditions (the most active drug for the treatment of ovarian cancer) in order to enlarge the scope of available drugs to cancer treatment. The camphor sulphonylimine Ag(I) complexes have the additional attractive to foresee the possibility of combined anticancer and antimicrobial activities, since $[Ag(NO_3)(^{III}L)]_n$ (**3**) was shown to have relevant antimicrobial properties. [4]

2. Results and discussion

2.1. Synthesis and characterization

Silver complexes with ligand to metal ratios ranging from 2:1, 1:1 or 1:2 were synthesized by reaction of silver nitrate ($AgNO_3$) with camphorsulphonylimines ($SO_2NC_{10}H_{13}NY$, Fig. 1) under experimental conditions selected to improve selectivity in the desired compound.

The complexes were formulated based on elemental and spectroscopic data (FTIR, NMR) and in the case of $[Ag(NO_3)(^{I}L)_2]$ (**1**; ^{I}L = $SO_2NC_{10}H_{13}NN(CH_3)_2$; Fig. 1) structural characterization by X-ray diffraction analysis was achieved (Fig. 2). $[Ag(NO_3)(^{I}L)_2]$ crystallizes in the Monoclinic C2 space group with a ML'$_2$ triangular geometry assuming a chalice-type shape (Fig. 2, inset). The silver atom, the nitrate (NO_3^-) nitrogen atom and the non-coordinated oxygen atom all lie in a crystallographic C2 axis making the two camphorsulphonylimine ligands symmetry related. These ligands bind silver through the nitrogen atom of the sulphonylimine group (=*N*SO_2) with the imine nitrogen atom of the hydrazone group (=*N*NMe_2) pointing to silver at a close non-bonding distance (2.765 Å), such as in the Pd(II) complexes [24]. DFT (Density Functional Theory) calculations for the Ag1 and the Ag2 centres (Fig. 2) as well as for the optimized structure (gas phase) confirm the non-bonding character of the silver-imine (Ag-*N*NMe_2) interaction with an overlap population (a parameter directly related to bond strength) considerably lower (3 to 4 times) than that for the silver-sulphonylimine (Ag-NSO_2) bond [respectively, 0.017 (Ag1… N), 0.024 (Ag2… N), 0.013 Ag… N vs 0.049, (Ag1… N), 0.068 (Ag2… N)] and 0.052 for the gas phase. The Ag—N bond length, in the gas phase is within the experimental error for the Ag2 centre (2.70 pm). The nitrate group completes the coordination sphere of silver acting as a bidentate ligand through the two oxygen atoms. Two molecules *per* unit exist as depicted in Fig. 2. Table 1 displays selected bond lengths and angles for **1**.

Under the appropriate experimental conditions complex $[(AgNO_3)_2(^{II}L)]$ (**2**, ^{II}L = $SO_2NC_{10}H_{13}NN(C_6H_5)_2$, Fig. 1) was synthesized with the metal to ligand ratio (2:1) opposite to **1** (1:2). The new ligand (^{II}L) was obtained by condensation of diphenylhydrazine with 3-oxocamphorsulfonylimine ($SO_2NC_{10}H_{13}O$) following the general procedure

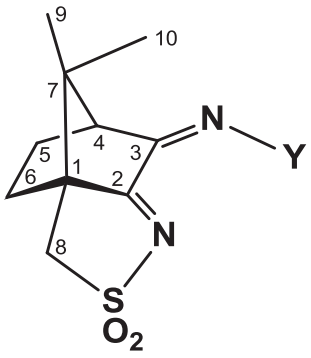

Fig. 1. Camphorsulphonylimine compounds used as ligands (Y = NMe_2, ^{I}**L**; Y = NPh_2, ^{II}**L**; Y = Ph, ^{III}**L**).

used for the synthesis of camphorsulphonylimine derivatives (see Experimental section). Structural characterization by X-ray crytallography shows that two molecules *per* asymmetric unit cell of ^{II}L exist, the compound assuming the *E*-configuration (Fig. 3).

Complexes **1** and **2** have similar spectroscopic properties (IR, NMR) despite inverse ligand/metal ratios (in **1** two ligands *per* metal exist while in **2** two metals *per* ligand exist). In the NMR spectra, the main difference is observed for the [13] C chemical shift of the imine carbon atom (C3, see Fig. 1 for numbering) that in **2** displays a value (140.1 ppm) ca. 8 ppm higher than in **1** (see experimental section). Such effect is conceivably due to additional binding of one of the nitrogen atoms of the hydrazone group (=*N*NPh_2) to $AgNO_3$, since two silver units exist *per* ligand. Deshielding is even greater in the coordination polymer $[Ag(NO_3)(^{III}L)]_n$ (**3**, ^{III}L = $SO_2NC_{10}H_{13}NC_6H_5$; C3, 169.3 ppm)[4] where outer sphere interactions are feasible. Complexes **1**, **2** and **3** have in common the $AgNO_3$ metal core and camphorsulphonylimine ligands which differ in the substituent (Y, Fig. 1). In **1** and **2**, the camphor substituent is of the hydrazone type (=*N*NR) while in **3** it is of the imine type (=NR). Whether these differences have a significant effect on the electronic properties of the complexes was surveyed by studying the redox properties of the complexes.

2.2. Redox properties

The redox properties of compounds are highly relevant in the way they interact with biological molecules, since electron transfer processes commonly occur. Thus, the study of the electrochemical behavior and measurement of the potentials at which the compounds reduce or oxidize may allow a better understanding of their interactions with DNA [25] and their biological activity. The electrochemical behavior of the compounds was studied by cyclic voltammetry in acetonitrile, a solvent where **1**–**3** are readily soluble and that allows a wide window of potentials to be observed. Data is displayed in Table 2.

All complexes (**1**–**3**) display one irreversible cathodic wave within a narrow range of potentials ($^{I}E_p^{red}$, Table 3) attributed to $Ag^+ \rightarrow Ag^0$ reduction. In the reverse scan a strong adsorption wave due to Ag^0 is observed. Such behavior, as well as the potentials ($^{I}E_p^{red}$, Table 3), does not differ much from that of $AgNO_3$ (E_p^{red} = 0.18 Volt).[4] The complexes display additional reversible cathodic ($^{II}E_{1/2}^{red}$, Table 3) and irreversible anodic waves ($^{III}E_p^{ox}$, Table 3) attributed to processes based on the ligands. The potentials of the cathodic process at the free camphorsulphonylimine compounds ($E_{1/2}^{red}$: ^{I}L, −1.50 V; ^{II}L, −1.32 V and ^{III}L, −1.16 V[4]) are similar to those measured for the coordinated ligands, while the potentials of the anodic processes in the free ligands (E_p^{ox}: ^{I}L, 1.34 V; ^{II}L, 1.28 V and ^{III}L, 1.82 V[4]) display higher potential values. Such trends suggest that the camphorsulphonylimine ligands essentially withdraw electron density from the metal, thus facilitating reduction of Ag(I). This effect is less pronounced for the hydrazone sulphonylimine (Y = NNR; **1** and **2**) than for the imine sulphonylimine complexes (Y = NR; **3**). The opposite effect (charge transfer from the ligand to the metal) is considered responsible for the Ag(I)→ Ag(0) process not having been observed in the phenolic hydrazone Ag(I) complex, and in the case of the related phenolic thiosemicarbazone Ag(I) complex (−0.14 V) the potential is considerably lower [26] than the values herein reported.

To get insight in the electrochemical behavior of the complexes (in non-aqueous medium) in the presence of calf thymus DNA (CT-DNA) a few drops of a CT-DNA solution (1 mg/mL, in H_2O) were added to the electrochemical cell and the process followed by cyclic voltammetry. A shift to lower values (ca. 30 to 57 mV) in the potential of the $Ag^+ \rightarrow Ag^0$ process was observed in all cases (wave **I**, Fig. 4). According to Bard such trend may be attributed to electrostatic interactions (groove binding) of the complexes with DNA. [27] Changes in the potentials and intensity of redox waves have been used to ascertain the type of interaction and binding constants, respectively. [28].

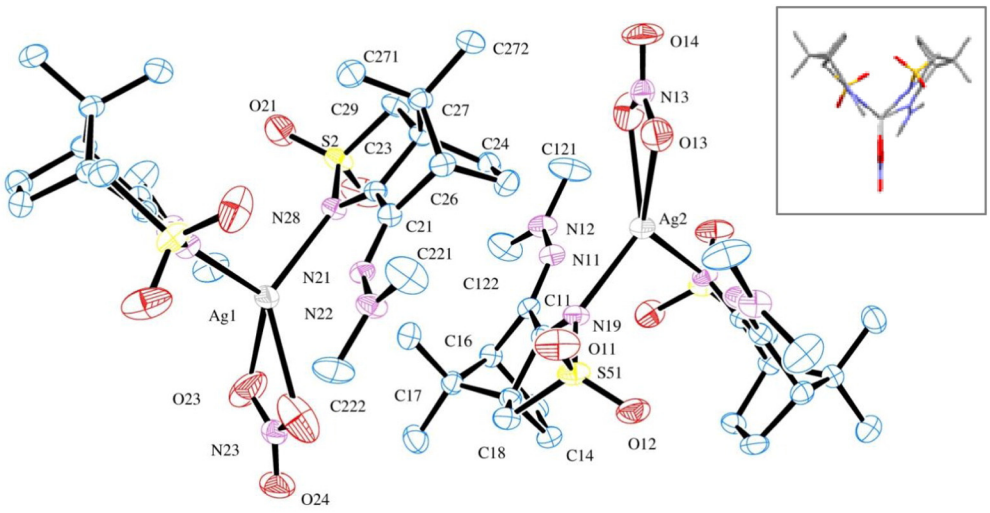

Fig. 2. ORTEP drawing for **1** showing the atom labeling scheme. Ellipsoids were drawn at 50% probability. Inset: Chalice type arrangement.

In the case of complexes **1** and **3**, no appreciable variation in the current intensity was found, while for compound **2** an increase in the intensity of the cathodic wave was observed (I, Fig. 4b) in contrast with a typical decrease. [29–31].

In the cyclic voltammogram of complex **1** (in the presence of CT-DNA) two additional waves (**a** and **b**) accompany a shift to higher potentials of the cathodic process **II** and the anodic wave **III** reveals as two overlaid waves (both anodic and cathodic processes considered as being based on the ligand) (Fig. 4 a).

At this stage the only clear evidence is that all complexes bind to DNA and that the type of interaction established by complex **1** is different from that of complexes **2** and **3**. Such observation was corroborated through fluorimetric studies (see below).

2.3. Cytotoxic activity

A time dependent study of the anticancer activity of Ag(I) camphorsulphonylimine complexes (**1**–**3**) was made using A2780 and A2780cisR ovarian cancer cells. Cells were exposed to increasing concentrations of complexes (0.01– 200 μM) during 3 h, 24 h and 48 h, at 37 °C. The IC_{50} values were calculated using the MTT assay (MTT = 3-(4,5-dimethylthiazol-2-yl)-2,5-diphenyltetrazolium bromide), which measures the reductase activity in the live cells. The compounds were first solubilized in DMSO keeping the amount of DMSO at values with no cytotoxic effect, even for the highest amounts (<1% in the cell medium).

The experimental data shows that the cytotoxic activity of the complexes varies with the incubation time and the complexes are considerably more active than *cisplatin* (lower IC_{50} values) in all cases. *Cisplatin* displays no activity for 3 h incubation time at concentrations up to 200 μM (Fig. 5). It is worth to highlight that the Ag(I) camphorsulphonylimine complexes (**1**–**3**) display activity towards the *cisplatin* resistant cells (A2780cisR) which is even higher than towards the sensitive cells (A2780), in agreement with a remarkable ability to overcome *cisplatin* resistance (Fig. 5).

In addition to time variation (3 h, 24 h and 48 h), a systematic study including the evaluation of the IC_{50} values for the non-tumoral cell line HEK 293 (human embryonic kidney), $AgNO_3$ and the camphorsulphonylimine compounds (used as ligands, ^{I}L-^{III}L) was made for the A2780 cells after 48 h incubation.

The activity of $AgNO_3$ and *cisplatin* are of the same order of magnitude being much lower than that of the complexes (**1**–**3**), whereas none of the ligands display cytotoxicity (IC_{50} > 100 for ^{I}L and ^{III}L and IC_{50} > 200 for ^{II}L) towards the A2780 cells (Table 3). Such data shows there is a relevant enhancement of the anti-proliferative activity due to the synergetic effect of combining silver nitrate and camphorsulphonylimines in the complexes.

The selectivity indexes (SI) for the complexes (**1**–**3**) and for cisplatin (Table 3) were calculated through the ratio of the IC_{50} values for the non-tumor cell line (HEK 293) and the corresponding IC_{50} values for each cancer cell line.

The cytotoxic effect of the complexes for the human embryonic kidney HEK cells is considerably high, although lower than for the tumor cells. The calculated selectivity indexes (SI) show that the complexes are ca. one order of magnitude more selective (19 > SI > 6.3) for the ovarian tumor cell lines than *cisplatin* (1.7 > SI > 0.47) (Table 3).

In order to get some insights into the mechanism of action and possible cellular targets, the NR (NR = 3-amino-7-dimethylamino-2-methylphenazine hydrochloride) assay was used as another in vitro cytotoxicity method. The NR and MTT assays are based on different physiological endpoints, although both measure parameters indicative of the degree of cell death. The NR assay is based on the incorporation of a weak cationic dye in the lysosomes of viable cells. Accordingly, cellular viability is a measure of lysosomal integrity. [33] Short incubation times are recommended for the NR assay therefore both assays were performed after 3 h treatment. The results show that the two assays display considerably different sensitivity for the Ag(I) complexes (Fig. 6) suggesting that the lysosomes may be the target for the complexes.

It is noteworthy that in the case of $AgNO_3$ a completely different mechanism seems to operate, since similar results are obtained through both assays (MTT and NR, Fig. 6).

Table 1
Selected bond lengths and angles for **1**.

Bond lengths (Å)		Angles (deg)	
Ag1—N28	2.398 (5)	N28—Ag1—N28[a]	102.1 (3)
Ag2—N19	2.460 (5)	N19—Ag2—N19[b]	103.5 (3)
Ag1—O23	2.623 (5)	O23—Ag1—O23[a]	48.1 (2)
Ag2—O13	2.476 (5)	O13—Ag2—O13[b]	49.1 (2)
N23—O23	1.237 (7)	O23—Ag1—N28	122.4 (2)
N23—O24	1.21 (1)	O13—Ag2—N19	114.1 (2)
N13—O13	1.251 (7)	N11—Ag2—N11[b]	132.8 (2)
N13—O14	1.22 (1)	N21—Ag1—N21[a]	138.2 (2)
Ag2… N11	2.69 (1)	N19—Ag2—N11	68.4 (2)
Ag1… N21	2.76 (1)	N28—Ag1—N23	67.7 (2)

[a] −x + 1,y,−z + 1.
[b] 2 −x,y,−z.

2.4. Study of interactions with DNA by fluorescence

To try to get further insight into the biological processes the binding ability to CT-DNA of the complexes (**1**–**3**) was evaluated.

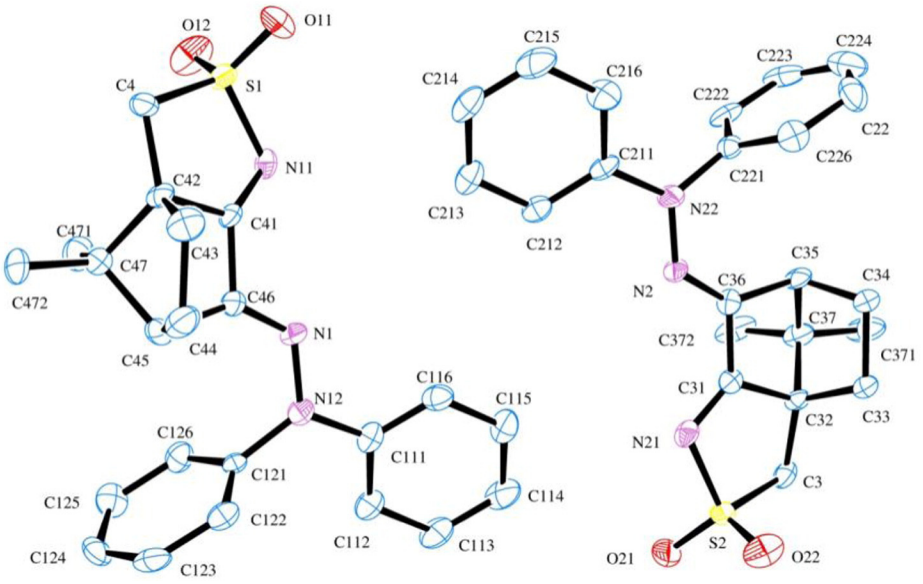

Fig. 3. ORTEP drawing of $SO_2NC_{10}H_{13}NN(C_6H_5)_2$ (^{II}L), showing the atom labeling scheme. Ellipsoids were drawn at 50% probability. Relevant bond lengths (Å): C46—N1, 1.295 (7); C36—N2, 1.295 (7); N1—N12, 1.364 (7); N2—N22, 1.336 (7) and angles (deg): C46—N1—N12, 122.1 (5); C36—N2—N22, 123.9 (5); C121—N12—C111, 120.5 (5); C211—N22—C221, 119.8 (5).

Fluorescence studies are commonly used to assess the binding affinity of compounds to DNA. Since the silver complexes **1**–**3** do not show fluorescence by themselves, the evaluation of the binding to DNA was done by competition studies. Ethidium bromide (EB), thiazole orange (TO), as well as other known intercalators could be used in competitive binding to DNA to probe intercalation. Although EB has been widely used, it is very toxic and mutagenic, a reason to choose TO, which is less toxic and furthermore exhibits higher, less sequence dependent affinity for DNA, generating a higher fluorescence enhancement upon binding to duplex DNA. [34] The study started by evaluating the best TO:DNA ratio to maximize the TO fluorescence emission, which under the experimental conditions used (PBS buffer 0.10 M, pH 7.4, 2.5 μM CT-DNA) was found to be TO:DNA = 0.9. The herein data was obtained upon excitation at 509 nm, the value at which TO displays excitation and emission fluorescence. The fluorescence spectra measured without TO (at different DNA:complex ratios) were subtracted from those containing the complex (DNA:TO:complex) and plotted (Fig. 7). In the case of complex **2**, precipitation inhibited studies with complex:DNA molar ratios above ca. 0.5. In all cases, a moderate fluorescence quenching is observed (ca. 40, 35 and 35%, respectively for complexes **1**, **3**, and **2**) indicating that the complexes interact with DNA either competing with TO for the same binding sites, or binding to different sites.

The experimental quenching data was analyzed with the Stern–Volmer equation. While data for compounds **2** and **3** adjusts roughly linear plots over all the range of concentrations, data for compound **1** shows a downward curvature (Fig. 8) pointing to, two different binding regions or competing binding modes. [36,36] The distinct characteristics of the fluorescence data obtained for **1** and the other complexes (**2** and **3**) parallels that observed by cyclic voltammetry, supporting different interactions with DNA.

The K_{SV} values (Table 4) show that the affinity of compound **2** for CT-DNA is one order of magnitude higher than that of complex **3**, a result that is in line with the cytotoxic activity observed for cells A2780 (Table 3).

The binding constant (K_a) and the number of binding sites *per* DNA molecule (n) were calculated from the plot of log[$(I_0 - I)/I$] versus log[complex] (Fig. 9) using the linear correlation log[$(I_0 - I)/I$] = logK_a + nlog[complex]. The K_a and the n values obtained are listed in Table 4.

From the data on Table 4, we can conclude that complex **2** ([{Ag(NO_3)}$_2$(^{II}L)]) with two metal units ($AgNO_3$) *per* ligand is the one that shows higher affinity to DNA. Complex **3** (metal to ligand 1:1) displays a K_a value 10 times lower than **2** (1.61×10^5 M^{-1}) and complex **1** (metal to ligand 1:2) displays very low affinity for DNA (1.07×10^1 M^{-1}, Table 4). The number of binding sites is ca. 1 for complexes **2** and **3** while it is ca. 0.3 for **1**. K_a and *n* were obtained from a double log equation, which linearizes non-linear data, and more importantly the equation only yields the binding stoichiometry for "infinite"

Table 2
Cyclic voltammetry data[a] for complexes **1**–**3** in NBu_4BF_4/CH_3CN (0.10 M).

Complex		Reduction (V)		
		$^{I}E_p^{red}$	$^{II}E_{1/2}^{red}$	$^{III}E_p^{ox}$
[Ag(NO_3)(^{I}L)$_2$][b]	**1**	0.17	−1.49	1.35[c]
[{Ag(NO_3)}$_2$(^{II}L)][d]	**2**	0.15	−1.35	1.30
[Ag(NO_3)(^{III}L)][4]	**3**	0.13	−1.16	1.77

[a] Values in volts (±10 mV) vs. saturated calomel electrode (SCE).
[b] $[Fe(\eta^5\text{-}C_5H_5)_2]^{0/+}$ ($E_{1/2}^{ox} = 0.382$ V) was used as internal reference.
[c] A shoulder is observed at $E_p^{ox} = 1.24$ V.
[d] Camphorphenazine ($E_{1/2}^{red} = -1.99$ V) was used as internal reference. A third irreversible reduction wave is observed at −1.85 V.

Table 3
Calculated IC_{50} for cell lines displayed and SI values[a] for the Ag(I) complexes (**1**–**3**), $AgNO_3$ and *cisplatin*, at 48 h incubation time.

Compounds		IC_{50} (μM)		
		A2780	A2780cisR	HEK 293
[Ag(NO_3)(^{I}L)$_2$]	**1**	1.11 ± 0.26	1.17 ± 0.22	9.1 ± 3.0
[{Ag(NO_3)}$_2$(^{II}L)]	**2**	0.65 ± 0.17	0.67 ± 0.19	4.2 ± 1.1
[Ag(NO_3)(^{III}L)]	**3**	0.76 ± 0.29	0.51 ± 0.10	9.9 ± 2.6
Ag(NO_3)		16.1 ± 0.3	–	–
cisplatin		20.7 ± 5.6	75.4 ± 30.0 [32]	35.5 ± 15.5 [16]
SI (**1**)		8.2	7.8	–
SI (**2**)		6.5	6.3	–
SI (**3**)		13	19	–
SI (**cis**)		1.7	0.47	–
IC_{50} (**1**)/IC_{50} (**cis**)		0.05	0.02	0.26
IC_{50} (**2**)/IC_{50} (**cis**)		0.03	0.009	0.12
IC_{50} (**3**)/IC_{50} (**cis**)		0.04	0.007	0.27

[a] The selectivity index (SI) of the complexes is given by the ratio of the IC_{50} values of the non-tumor cells (HEK 293) versus the IC_{50} for the cancer cells.

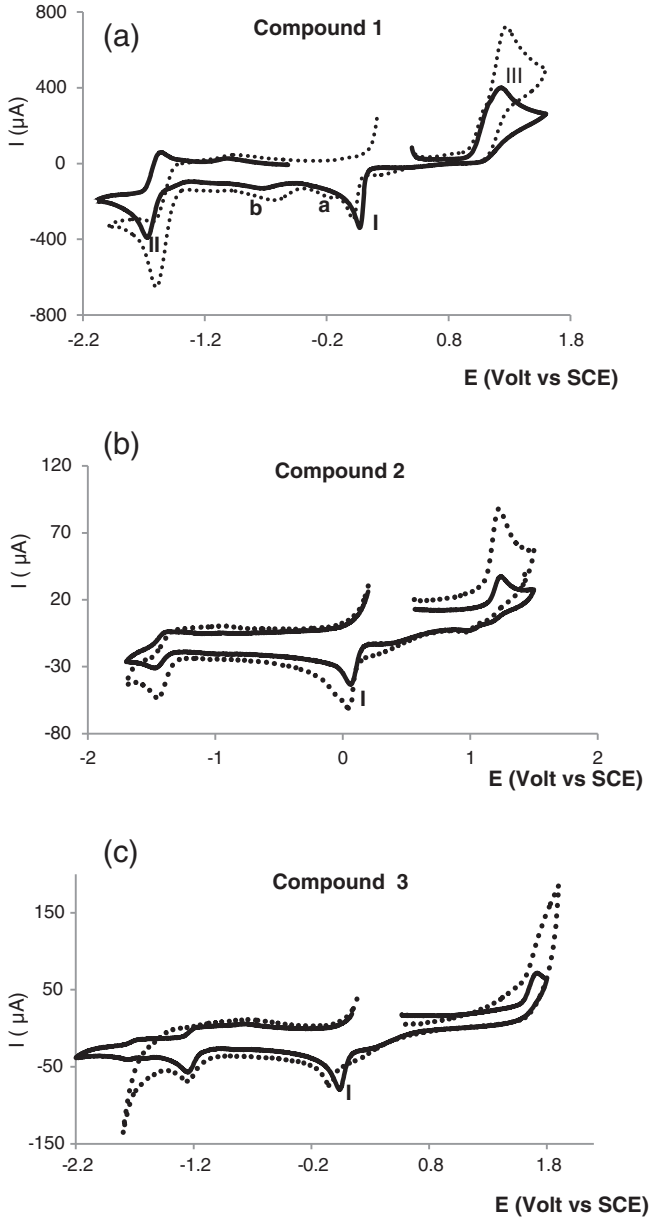

Fig. 4. Cyclic voltammograms of the camphorsulphonylimine complexes obtained in 0.1 M Bu_4NBF_4/CH_3CN using a Pt wire electrode: in the absence of CT-DNA (—) or upon addition of a few drops of CT-DNA (....).

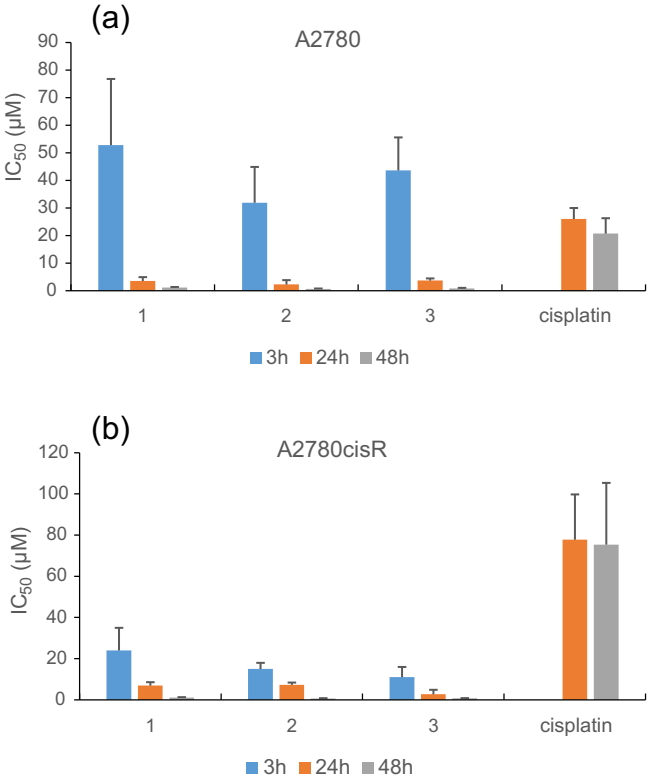

Fig. 5. Time dependent cytotoxic activity (IC_{50}) evaluated through the MTT assay on the ovarian cells: (a) A2780 and (b) A2780cisR.

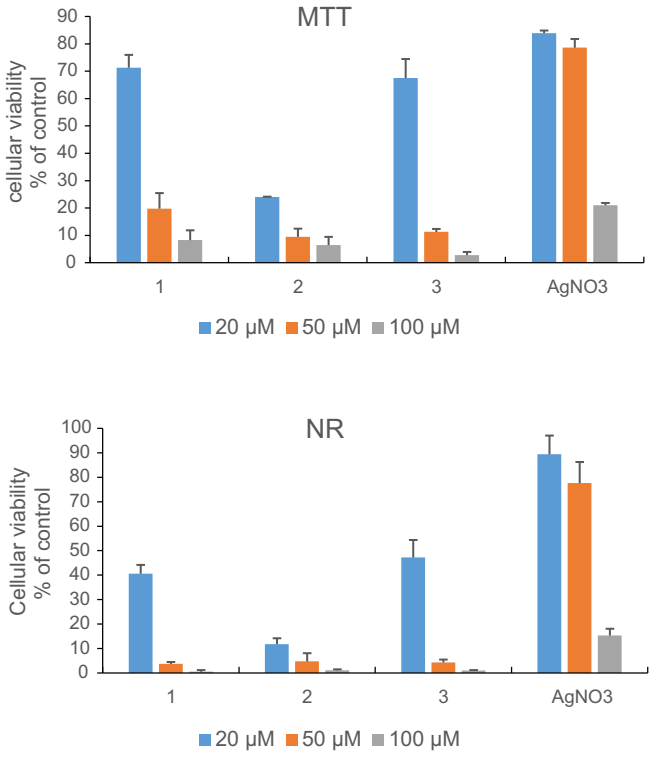

Fig. 6. Comparison of the MTT and Neutral Red (NR) methods for assessment of different endpoints of the cytotoxic activity of the compounds against the A2780 cells upon 3 h incubation. (For interpretation of the references to colour in this figure legend, the reader is referred to the web version of this article.)

cooperativity; i.e., the occupation of one binding site favours the binding of other ligands, which is a very unrealistic hypothesis. When the hypothesis of "infinite" cooperativity is not satisfied, *n* is just a phenomenological parameter (the Hill coefficient), which is lower than the real number of binding sites. [37].

For comparative purposes, the ability of $AgNO_3$ and ^{II}L to quench TO was also evaluated. The data obtained is consistent with no ability of $AgNO_3$ to quench TO fluorescence and the ligand (^{II}L) shows very low quenching ability (see supplementary information).

The ability to quench the TO fluorescence implies that complexes **2** and **3** are able to compete with TO for the same binding sites, or interact with DNA at different sites. However, we cannot conclude if the binding involves intercalation or if it is simply through electrostatic or hydrogen bonding interactions. Although the binding order is the same as found e.g. in the cell studies with A2780, **2** > **3** > **1**, the magnitude of K_a is quite different and the binding constant cannot be correlated with the cytotoxic activity of the complexes.

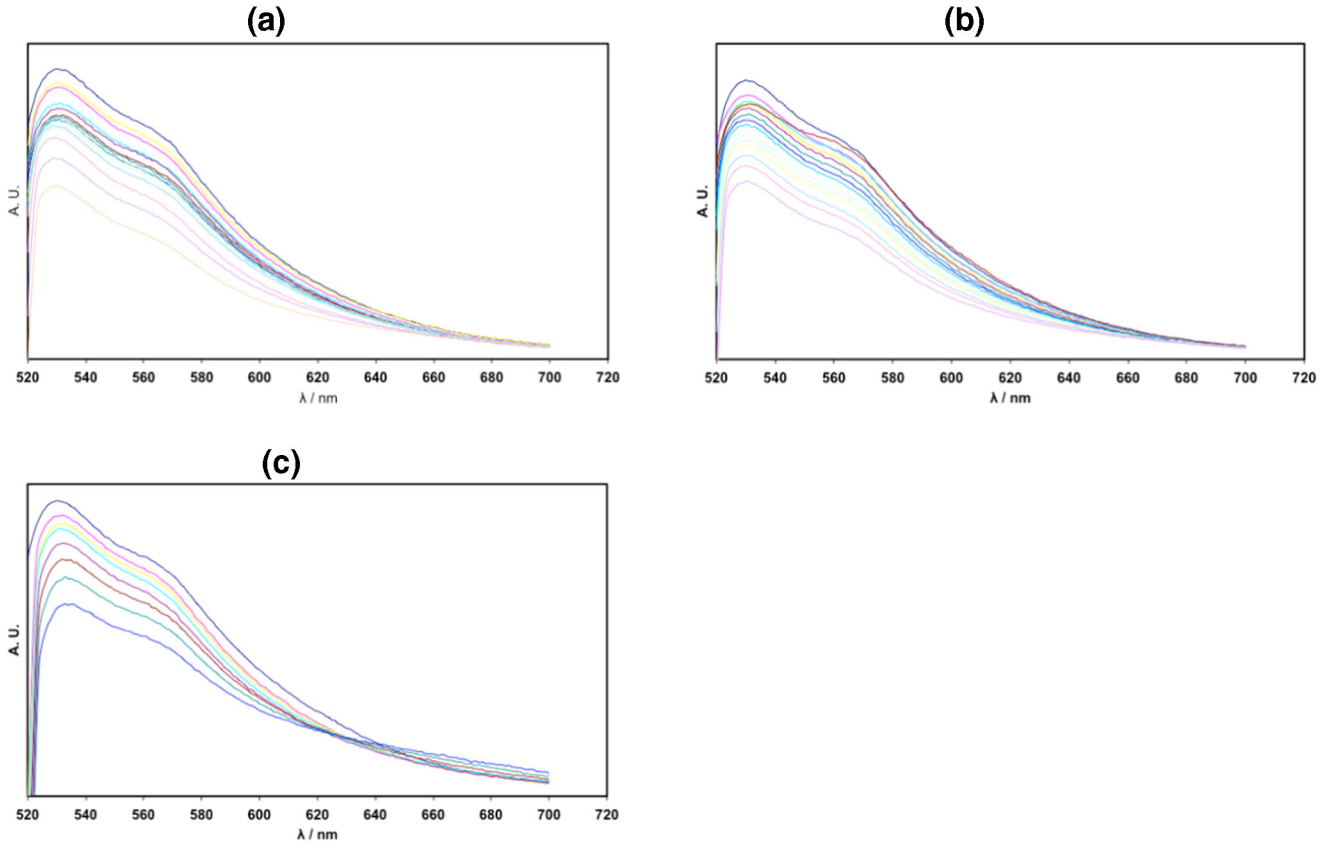

Fig. 7. – Fluorescence emission spectra after subtraction of the blank spectra (excitation at 509 nm and slits 7 nm). a) [DNA] = 2.57 μM and [**1**] = 0–21 μM; b) [DNA] = 2.68 μM and [**2**] = 0–2.0 μM; c) [DNA] = 2.57 μM and [**3**] = 0–23 μM. In all cases the fluorescence intensity decreases with increasing Ag-complex concentration.

3. Conclusions

Two novel Ag(I) camphorsulphonylimine complexes ([$Ag(NO_3)(^{I}L)_2$], **1**; [$(AgNO_3)_2(^{II}L)$], **2**) were synthesized and analytically and spectroscopically characterized including structural characterization by X-ray diffraction analysis in the case of [$Ag(NO_3)(^{I}L)_2$].

The anti-proliferative properties of the new complexes as well as those of [$Ag(NO_3)(^{III}L)$] (**3**, that covers the 1:1 metal to ligand ratio) were assessed against the human ovarian *cisplatin*-sensitive A2780 and *cisplatin*-resistant A2780cisR using the MTT assay. All complexes display IC_{50} values (1.11-0.65 μM for A2780; 1.17-0.51 μM for A2780cisR) at least one order of magnitude lower than *cisplatin* (20.7 ± 5.6 μM for A2780) in agreement with considerably higher cytotoxic properties. The IC_{50} value (16.1 ± 0.3 μM for A2780) obtained for silver nitrate is similar to that of *cisplatin* while the ligands display values very high (IC_{50} > 100 μM) in agreement with no cytotoxic

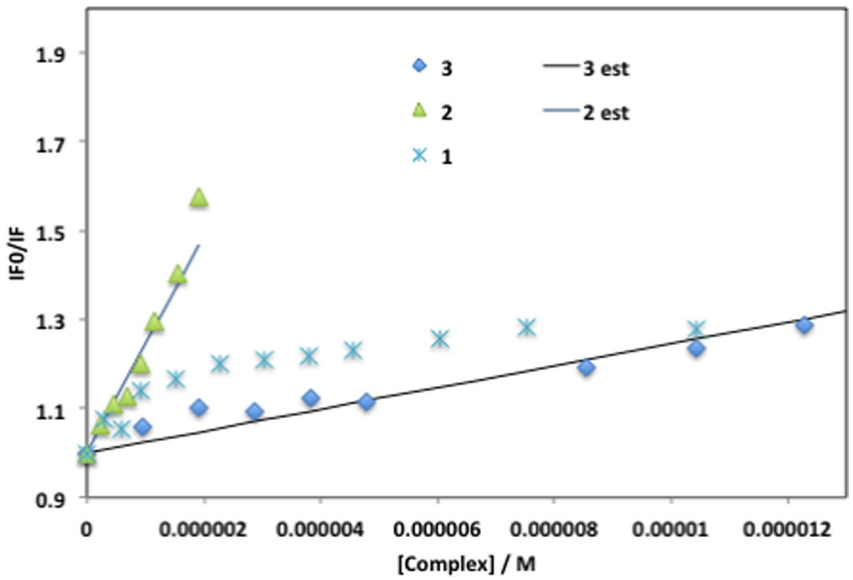

Fig. 8. Stern–Volmer plots at 529 nm obtained from steady-state (I_0/I). Excitation at 509 nm and slits 7 nm. I_0/I data was corrected for inner-filter-effects.

Table 4
Stern–Volmer constant (Ksv), binding constant (K_a) and n binding sites calculated for the interaction of complexes **1**-**3** with CT-DNA[a].

Compound	$K_{SV}(M^{-1})$	$K_a\ (M^{-1})$	n
1	–	1.07×10^{1}	0.31
2	2.44×10^{5}	1.61×10^{5}	0.95
3	2.45×10^{4}	2.54×10^{4}	1.00

[a] CT-DNA (2.5 μM) in PBS (0.1 M, pH 7.4).

activity. Complexes **2** and **3** (with 2:1 and 1:1, metal to ligand ratios, respectively) display similar IC_{50} values, although with an inverse order in what concerns cell lines A2780 and A2780cisR, i.e. [Ag(NO_3)(^{III}L)] displays the lowest IC_{50} value (0.65 ± 0.17 μM) for cell line A2780, and [Ag(NO_3)(^{III}L)] displays the lowest IC_{50} value (0.51 ± 0.10 μM) for cell line A2780cisR. Complex [Ag(NO_3)(^{I}L)$_2$] with the highest content in ligand (2:1) displays slightly higher IC_{50} values than **2** and **3** for both cell lines (1.11 ± 0.26 μM for A2780 and 1.17 ± 0.22 for A2780cisR). The complexes (**1**–**3**) display cytotoxic activity towards the non-tumoral human embryonic kidney HEK 293 cell line considerably high, although lower than against the cancer cell lines A2780 and A2780cisR.

The use of two methods (MTT and NR assays) based on different endpoints of cytotoxicity to evaluate the activity of the compounds, lead to the conclusion that the mechanism of action of the complexes differs from that of the silver precursor ($AgNO_3$).

The interaction of the complexes with CT-DNA was studied by fluorescence and cyclic voltammetry showing that the complexes (**1**–**3**) bind to DNA, although the mechanism is not necessarily the same for all complexes. Data from fluorescence quenching shows that complex **2** has the highest affinity to DNA ($K_a = 1.61 \times 10^5\ M^{-1}$) and that binding of **1** to CT-DNA follows a mechanism different from that of complexes **2** and **3**, a fact also supported by cyclic voltammetry. According to cyclic voltammetry data electrostatic interactions (groove binding) are responsible for binding to DNA.

In conclusion, the three silver camphorsulphonylimine complexes have promising anti-cancer activities, although their cytotoxicity towards HEK 293 cell line is by now a drawback on a possible therapeutic use. A step forward will be tuning of the characteristics of the sulphonylimine camphor ligands by replacement of the imine substituent (Y) to overcome toxicity for healthy cell lines. Additionally, there is an auspicious possibility of combining the high anti-proliferative activity of complex **3** (the less toxic for healthy cells) against cancer cell lines (A2780; A2780cisR) with its antibacterial properties (previously reported) to control infections by Gram-negative strains in some cases accompanying cancer treatment.

4. Experimental

All complexes were prepared under nitrogen atmosphere using vacuum/Schlenk techniques. Complex **3** and ligand ^{I}L were prepared according to published procedures. [4,24] (+)-Camphor-10-sulfonic acid, 1,1-dimethyl hydrazine and 1,1-diphenyl hydrazine hydrochloride were purchased from Sigma-Aldrich. The solvents (PA grade) are acetonitrile from Carlo Erba and all the others are from Panreac. IR spectra were obtained from KBr pellets using a JASCO FT/IR 4100 spectrometer. NMR spectra (^{1}H, ^{13}C, DEPT, HSQC and HMBC) were obtained from acetone-d_6 or acetonitrile-d_3 solutions using Bruker Avance II$^+$ (300 or 400 MHz) spectrometers. NMR chemical shifts are referred to TMS (δ = 0 ppm). Cyclic voltammograms (CV) were obtained from Bu_4NBF_4/CH_3CN (0.10 M) solutions using a three compartments cell equipped with platinum wire working and secondary electrodes interfaced with a VoltaLab PST050 equipment. The potentials were measured in Volts (± 10 mV) versus SCE at 200 mV/s using (Fe(η^5-C_5H_5)$_2$]$^{0/+}$ ($E^{red}_{1/2}$0.382 V) as internal reference. UV–Visible absorption (UV–Vis) spectra were recorded on a Perkin-Elmer Lambda 35 spectrophotometer at room temperature. Fluorescence spectra were measured on Horiba Jobin Yvon fluorescence spectrometer model FL 1065 at room temperature. Millipore water was used for the preparation of Phosphate Saline Buffer (PBS) (0.10 M, pH = 7.4). Acetonitrile was used for the preparation of the stock solutions of the complexes. Calf Thymus DNA (CT-DNA) was purchased from Sigma (#D3664) and used as received.

5. Synthesis

5.1. Ligand

(*Z*)-7-(2,2-diphenylhydrazono)-8,8-dimethyl-4,5,6,7-tetrahydro-3*H*-3a,6-methanobenzo [*c*]isothiazole 2,2-dioxide (**^{II}L**) - 1,1-diphenylhydrazine hydrochloride (1.30 g; 6.0 mmol) was added to NaOAc (0.50 g; 6.0 mmol) in 10 mL of EtOH and stirred at room

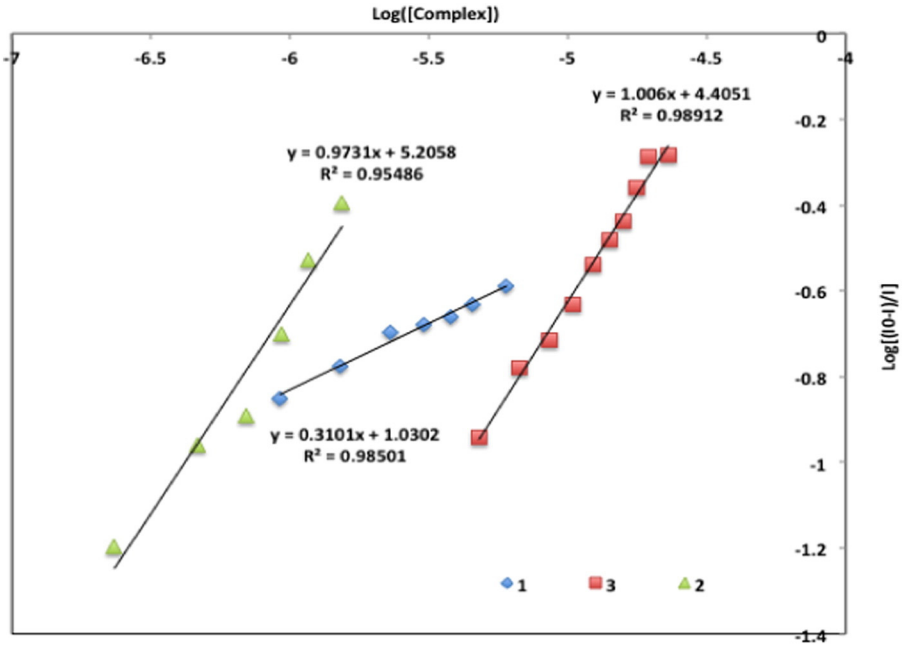

Fig. 9. Plot of log ($I_0 - I$)/I vs. log [Complex] for all systems. [CT-DNA] = 2.7 μM, [TO] = 2.47 μM, [**1**] = 0–6.0 μM, [**2**] = 0–1.6 μM, [**3**] = 0–2.3 μM.

temperature for 1 h. 3-oxo-camphorsulfonimide (0.46 g; 2.0 mmol) was then added and stirred at room temperature for 72 h. After solvent removal, the orange oil was re-dissolved in dichloromethane (50 mL) and washed with water (3 × 25 mL). The organic layer was dried with $MgSO_4$, filtered and the dichloromethane was evaporated, affording a dark yellow solid. Yield 62%. IR (cm^{-1}): 1618 (ν_{CNN}), 1587 (ν_{CN}), 1320 (ν_{SO2}, ass*ym*), 1134 (ν_{SO2}, sym). Elem. Anal. (%) for $C_{22}H_{23}N_3O_2S{\cdot}0.1H_2O$ Found: C, 66.8; N, 10.6; H, 5.9; S, 8.1. Calc. C, 66.8; N, 10.7; H, 5.9; S, 7.8. ^{1}H NMR (acetone-d_6, δ ppm): 7.55–7.47 (m, 4H), 7.39–7.29 (m, 6H), 3.33, 3.14 (2d, J_{HH} = 13.6 Hz, 2H), 2.14–2.07 (m, 1H), 1.70–1.59 (m, 2H), 1.57–1.49 (m, 1H), 1.43 (d, J_{HH} = 4.4, 1H), 0.85 (s, 3H), 0.81 (s, 3H). ^{13}C NMR (acetone-d_6, δ ppm): 187.3 (C2), 145.4 (C_{ipso}), 140.1 (C3), 130.7, 127.3, 123.7 (C_{Ph}), 63.1 (*C*1), 51.7 (*C*4), 50.2 (C8), 48.0 (C7), 29.5 (C6), 24.7 (C5), 19.8, 18.6 (C9, C10).

5.2. Complexes

$[Ag(NO_3)(C_{12}H_{19}N_3SO_2)_2]$ (**1**) – Acetonitrile (10 mL) was added to a mixture of $AgNO_3$ (0.035 g, 0.21 mmol) and ^{I}**L** (0.10, 0.41 mmol) and the suspension was stirred overnight. A small quantity of brownish suspension formed which was filtered off and discarded. The solvent was reduced to ca. 4 mL and the solution left in the fridge for a few days until yellow crystals precipitated which were filtrated and dried under vacuum. Yield 75%. IR (cm^{-1}): 1616w, 1538 (υ_{CN}); 1384(υ_{NO3}); 1316 (υ_{SO2}). Elem. Anal. (%) for $AgC_{24}H_{38}N_7O_7S_2$: Found: C, 40.6; N, 13.9; H, 5.4; S, 9.0. Calc.: C, 40.7; N, 13.8; H, 5.4; S, 9.0. ^{1}H NMR: (CD_3CN, δ ppm): 3.32 (d, *J* = 2.1 Hz, 1H), 3.28 (s, 6H), 3.30, 3.08 (2d, *J* = 13.5 Hz, 2H) 2.14-2.10 (m, 2H), 1.67–1.60 (m, 2H), 1.01 (s, 3H), 0.87 (s, 3H). ^{13}C NMR (CD_3CN, δ ppm): 187.6 (C2), 132.5 (C3), 63.2 (*C*1), 52.7 (*C*4), 50.4 (C8), 49.3 (C7), 46.5 ($N(CH_3)_2$), 29.1, 26.7 (C5 + C6), 20.0, 19.0 (C9 + C10).

$[\{Ag(NO_3)\}_2(C_{22}H_{23}N_3SO_2)]$ (**2**) – A similar procedure to that described for **1** was used. $AgNO_3$ (0.034 g, 0.20 mmol); ^{II}**L** (0.10 g, 0.025 mmol). Yield 55%. IR (cm^{-1}): 1618w, 1534 (υ_{CN}); 1587 (CH_{arom}), 1384(υ_{NO3}); 1320 (υ_{SO2}). Elem. Anal. (%) for $Ag_2C_{22}H_{23}N_5O_8S$: Found: C, 36.3; N, 9.5; H, 3.2; S, 4.4. Calc.: C, 36.0; N, 9.6; H, 3.2; S, 4.4. ^{1}H NMR: (CD_3CN, δ ppm): 7.46 (t, *J* = 7.5 Hz, 2H), 7.33 (t, *J* = 7.4 Hz, 1H), 7.26 (d, *J* = 7.5 Hz, 2H), 3.35, 3.08 (2d, *J* = 13.7 Hz, 2H) 2.14–2.11 (m, 2H), 1.67–1.34 (m, 2H), 0.77 (s, 3H), 0.76 (s, 3H). ^{13}C NMR (CD_3CN, δ ppm): 188.4 (C2), 145.4 (Ph_{ipso}), 140.1 (C3), 130.8, 127.5, 123.7 (CH_{Ph}), 63.4 (C1), 51.7 (C4), 50.3 (C8), 48.3 (C7), 29.6, 24.7 (C5 + C6), 18.7, 18.5 (C9 + C10).

5.3. Crystallographic data

X-ray data for $[Ag(NO_3)(C_{12}H_{19}N_3SO_2)_2]$ (**1**) and $^{II}L = SO_2NC_{10}H_{13}NN(C_6H_5)_2$ was collected at 150 (2) K using a Bruker AXS-KAPPA APEX II area detector apparatus equipped with a graphite-monochromated Mo Kα (λ = 0.71073 Å) and were corrected for Lorentz polarization and, empirically, for absorption effects. The structures were solved by direct methods using SHELX97 [38] and refined by full matrix least squares against F^2 using SHELX97 all included in the suite of programs WinGX v1.70.01 for Windows . [39] The non-hydrogen atoms were refined anisotropically and the H atoms were inserted in idealized positions and allowed to refine riding on the parent atom. Rigid bond restrains were applied to all Ag—O bonds. Crystal data and refinement parameters are summarized in Table 5. Illustrations of the molecular structures were made with ORTEP3. [40].

Cambridge Crystallographic Data Centre (CCDC 1480542-1480543) contains the supplementary crystallographic data for this article. The X-ray data can be obtained free of charge via www.ccdc.cam.ac.uk/conts/retrieving.html (or from the CCDC, 12, Union Road, Cambridge CB2 1EZ, UK; fax: þ44 1223 336033 or deposit@ccdc.cam.ac.uk).

Table 5
Crystallographic data for: $[Ag(NO_3)(C_{12}H_{19}N_3SO_2)_2]$ (**1**) and $^{II}L = SO_2NC_{10}H_{13}NN(C_6H_5)_2$.

	1	^{II}L
Empirical formula	$C_{24}H_{38}N_7O_7S_2Ag$	$C_{44}H_{46}N_6O_4S_2$
Formula weight	708.60	786.99
Crystal system	Monoclinic	Monoclinic
Space group	C2	$P2_1$
Unit cell dimensions		
a/Å	12.723(1)	7.267(1)
b/Å	17.749(1)	17.211(3)
c/Å	13.452(1)	15.762(3)
α/deg	90	90
β/deg	103.577(4)	95.002(7)
γ/deg	90	90
Volume ($Å^{-3}$)	2952.7(4)	1964.0(6)
Z, Dcal (g/cm^3)	4, 1.594	2, 1.331
Absorption coefficient (mm^{-1})	0.879	0.188
F(000)	1464	832
Crystal size (mm^3)	0.3 × 0.2 × 0.3	0.3 × 0.3 × 0.4
θ range for data collection (deg)	1.56 to 26.33	1.30 to 26.43
Index ranges	−15 ≤ h ≤ 15, −22 ≤ k ≤ 21, −16 ≤ l ≤ 15	−9 ≤ h ≤ 9, −20 ≤ k ≤ 21, −19 ≤ l ≤ 19
Reflections collected / unique	18,320/5833 [R(int) = 0.0409]	11,430/7399 [R(int) = 0.0477]
Data/restraints/parameters	5834/1/381	7399/1/509
Final R (observed)	R1 = 0.0297, wR2 = 0.0701	R1 = 0.0753, wR2 = 0.2097

5.4. Computational calculations

DFT calculations were carried out using GAMESS-US [41] version *R*3 with a B3LYP functional using a SBKJC basis set.

5.5. Cytotoxic studies

Cells (ATCC) were grown in RPMI 1640 medium (A2780 and A2780cisR) or DMEM containing GlutaMax I (HEK 293) supplemented with 10% fetal bovine serum and were maintained in a humidified atmosphere of 5% CO_2. Cell viability was measured by the colorimetric MTT and Neutral Red (NR) assays which assessed active metabolic cells and lysosomal integrity, respectively. For a typical assay, cells were seeded in 96-well plates at a density of 1-2 × 10^4 cells/200 μL of appropriate medium and left to incubate approximately 24 h for optimal adherence. Compounds were previously diluted in DMSO and then in the medium. Maximum DMSO concentration in the medium was 1% (v/v). *Cisplatin* was first diluted in water and then in the medium. After careful withdraw of the medium, 200 μL of a serial dilution of compounds in fresh medium were added to the cells (six replicates per compound dilution) and incubation was carried out at 37 °C for several time points. At the end of the treatment and for the MTT assay the compounds were discarded and the cells were incubated with 200 μL of MTT solution in PBS (0.5 mg/ml). After 3–4 h at 37 °C the medium was removed and replaced by 200 μL of DMSO to solubilize the purple formazan crystals formed. The percentage of cellular viability was evaluated measuring the absorbance at 570 nm using a plate spectrophotometer (Power Wave Xs, Bio-Tek). The IC_{50} values were calculated by the GraphPad Prism software (version 5.0). Results are mean ± SD of at least two independent experiments done with six replicates. For the NR assay a commercial kit from Sigma-Aldrich was used. After treatment with the complexes 0.2 mL NR (0.33% in serum-free medium) was added to each well. The plates were incubated at 37 °C for a further 3 h. After incubation the cells were washed with NR assay fixative, and the incorporated dye was then solubilized in 0.2 mL of NR. The cellular viability was evaluated by measuring the absorbance at 540 nm.

5.6. DNA interactions

The experimental conditions were settled as follows: PBS buffer 0.10 M, pH 7.4 and ca. 2.5 μM CT-DNA. The DNA:TO ratio was optimized (TO:DNA = 0.9) in order to maximize the TO fluorescence emission. DNA stock solutions were prepared by dissolution in PBS buffer. The concentration of CT-DNA was determined by UV–Vis absorbance using the molar absorption coefficient at 260 nm (6600 M^{-1} cm^{-1}). The UV absorbance at 260 nm and 280 nm of the CT-DNA solution gave ratios of 1.8–1.9, indicating that the DNA was sufficiently free of protein. The stock solutions of the complexes and the camphorsulphonylimine ligand (^{II}L) were prepared in CH_3CN and $AgNO_3$ in Millipore water. All solutions were used within a few hours. The amount of organic solvent was kept below 5% (v/v). The fluorescence experiments were done using a quartz cuvette of 1 cm path length. Bandwidth was 7 nm in both excitation and emission. Fluorescence titrations were done by adding increasing amounts of the complexes (ca. 200-400 μM) to a solution containing thiazole orange (TO) and CT-DNA (0.9:1) ([DNA] ca. 2.5 μM). In the competition fluorescence titrations the DNA-TO samples were excited at 509 nm and the emitted fluorescence was recorded between 520 and 700 nm. UV–Vis absorption spectra were collected in all measured systems to correct the data for reabsorption and inner filter effects.[35,36] The concentrations were selected in order to have absorbance values below 0.2 at the excitation and emission wavelengths. Blank fluorescence spectra (containing everything except the fluorophore, TO) were measured and subtracted from each sample's emission spectra.

The quenching data was analyzed with the Stern–Volmer equation ($I_0/I = K_{SV}[Q] + 1$) where I_0 is the emission intensity in the absence of the quencher, I is the emission intensity in the presence of the quencher, K_{SV} is the quenching Stern–Volmer constant, and [Q] is complex concentration (quencher). The K_{SV} value is obtained as the slope from the plot of I_0/I versus [Q]. The K_{SV} constants for complexes **2** and **3** were obtained from the initial regions of the plots (I_0/I versus [Q], Fig. 9).

Acknowledgements

Financial support by FCT-Fundação para a Ciência e Tecnologia (UID/QUI/00100/2013, UID/Multi/04349/2013, RECI/QEQ-MED/0330/2012 and RECI/QEQ-QIN/0189/2012 and Investigador FCT) and the NMR Network (IST-UTL Node) for facilities.

Appendix A. Supplementary data

Supplementary data to this article can be found online at doi:10.1016/j.jinorgbio.2016.11.003.

References

[1] J.G. Leid, A.J. Ditto, A. Knapp, P.N. Shah, B.D. Wright, R. Blust, L. Christensen, C.B. Clemons, J.P. Wilber, G.W. Young, A.G. Kang, M.J. Panzner, C.L. Cannon, Y.H. Yun, W.J. Youngs, N.M. Seckinger, E.K.J. Cope, Antimicrob. Chemother. 67 (2011) 138–148.
[2] W.J. Youngs, A.R. Knapp, P.O. Wagers, C.A. Tessier, Dalton Trans. 41 (2012) 327–336.
[3] K.M. Fromm, Appl. Organometal. Chem. 27 (2013) 683–687.
[4] J.M.S. Cardoso, A.M. Galvão, S.I. Guerreiro, J.H. Leitão, A.C. Suarez, M.F.N.N. Carvalho, Dalton Trans. 45 (2016) 7114–7123.
[5] A.E. McRee, J. Exotic Pet Medicine 24 (2015) 240–244.
[6] B.S. Atiyeh, M. Costagliola, S.N. Hayek, S.A. Dibo, Burns 33 (2007) 139–148.
[7] S. Medici, M. Peana, G. Crisponi, V.M. Nurchi, J.I. Lachowicz, M. Remelli, M.A. Zoroddu Coord, 2016. Chem. Rev. http://dx.doi.org/10.1016/j.ccr.2016.05.015 (in press ASAP).
[8] C.N. Banti, S.K. Hadjikakou, Metallomics 5 (2013) 569–596.
[9] H.L. Zhu, X.M. Zhang, X.Y. Liu, X.J. Wang, G.F. Liu, A. Usman, H.K. Fun, Inorg. Chem. Commun. 6 (2003) 1113–1116.
[10] B. Thati, A. Noble, B.S. Creaven, M. Walsh, M. McCann, K. Kavanagh, M. Devereux, D.A. Egan, Cancer Lett. 248 (2007) 321–331.
[11] X.-J. Tan, H.-Z. Liu, C.-Z. Ye, J.-F. Lou, Y. Liu, D.-X. Xing, S.-P. Li, S.-L. Liu, L.-Z. Song, Polyhedron 71 (2014) 119–132.
[12] M.A. Iqbal, R.A. Haque, M.B. Khadeer Ahamed, A.M.S. Abdul Majid, S.S. Al-Rawi, Med. Chem. Res. 22 (2013) 2455–2466.
[13] S. Shukla, A.P. Mishra, J. Chem. (2013), 527123.
[14] J.J. Liu, P. Galettis, A. Farr, L. Maharaj, H. Samarasinha, A.C. McGechan, B.C. Baguley, R.J. Bowen, S.J. Berners-Price, M.J. McKeage, J. Inorg. Biochem. 102 (2008) 303–310.
[15] Y.-L. Li, Q.-P. Qin, Y.-F. An, Y.-C. Liu, G.-B. Huang, X.-J. Luo, G.-H. Zhang, Inorg. Chem. Commun. 40 (2014) 73–77.
[16] V. Gandin, M. Pellei, M. Marinelli, C. Marzanoa, A. Dolmella, M. Giorgetti, C. Santini, J. Inorg. Biochem. 129 (2013) 135–144.
[17] P.S. Brunetto, T.V. Slenters, K.M. Fromm, Materials 4 (2011) 355–367.
[18] T.V. Slenters, J.L. Sagué, P.S. Brunetto, S. Zuber, A. Fleury, L. Mirolo, A.Y. Robin, M. Meuwly, O. Gordon, R. Landmann, A.U. Daniels, K.M. Fromm, Materials 3 (3407) (2010) 3429.
[19] M. Varisco, N. Khanna, P.S. Brunetto, K. Fromm, ChemMedChem 9 (2014) 1221–1230.
[20] Z.-C. Xiong, Y.-J. Zhu, F.-F. Chen, T.-W. Sun, Y.-Q. Shen, Chem. Eur. J. 22 (11224) (2016) 11231.
[21] A.S. Sokolova, O.I. Yarovaya, A.V. Shernyukov, M.A. Pokrovsky, A.G. Pokrovsky, V.A. Lavrinenko, V.V. Zarubaev, T.S. Tretiak, P.M. Anfimov, O.I. Kiselev, A.B. Beklemishev, N.F. Salakhutdinov, Bioorg. Med. Chem. 21 (2013) 6690–6698.
[22] L. Wang, S. Gou, Y. Chen, Y. Liu Bioorg, Med Chem. Lett. 15 (2005) 3417–3422.
[23] T.A. Fernandes, F. Mendes, A.P.S. Roseiro, I. Santos, M.F.N.N. Carvalho, Polyhedron 87 (2015) 215–219.
[24] M.F.N.N. Carvalho, L.M.G. Costa, A.J.L. Pombeiro, A. Schier, W. Scherer, S.K. Harbi, U. Verfürth, R. Herrmann, Inorg.Chem. 33 (1994) 6270–6277.
[25] M. Sirajuddin, S. Ali, A. Badshah, J. Photochem. Photobiol. B: Biology 124 (2013) 1–19.
[26] N.V. Loginova, T.V. Koval'chuk, A.T. Gres, N.P. Osipovich, G.I. Polozov, Y.S. Halauko, Y.V. Faletrov, H.I. Harbatsevich, A.V. Hlushko, I.I. Azarko, Y.V. Bokshits, Polyhedron 88 (2015) 125–137.
[27] A.J. Bard, M.T. Cater, M. Rodoriguez, J. Am. Chem. Soc. 111 (1989) 8901–8911.
[28] A. Shah, E. Nosheen, S. Munir, A. Badshah, R. Qureshi, N.M. Zia-ur-Rehman, H. Hussain, J. Photochem. Photobiol. B: Biol. 120 (2013) 90–97.
[29] F. Jalali, G. Rasaee, Int. J. Biol. Macromol. 81 (2015) 427–434.
[30] L. Fotouhi, Z. Atoofi, M.M. Heravi, Talanta 103 (2013) 194–200.
[31] P.S. Guin, P. Das, S. Das, P.C. Mandal, Int. J. Electrochem. (2012), 183745 (10 pages).
[32] I. Correia, P. Adão, S. Roy, M. Wahba, C. Matos, M.R. Maurya, F. Marques, F.R. Pavan, C.Q. Leite, F. Avecilla, J.C. Pessoa, J. Inorg. Biochem. 141 (2014) 83–93.
[33] G. Fotakis, J.A. Timbrell, Toxicol. Lett. 160 (2006) 171–177.
[34] J. Nygren, N. Svanvik, M. Kubista, Biopolymers 46 (1998) 39–51.
[35] A. Coutinho, M. Prieto, J. Chem. Educ. 70 (1993) 425–428.
[36] B. Valeur, Molecular Fluorescence, Principles and Applications, Wiley, Weinheim, 2001.
[37] M. van de Weert, L. Stella, J. Mol. Struct. 998 (2011) 144–150.
[38] G.M. Sheldrick, SHELX-97- Programs for Crystal Structure Analysis (Release 97-2), Institüt für Anorganische Chemie der Universität, Tammanstrasse 4, D-3400 Göttingen, Germany, 1998.
[39] L.J. Farrugia, WINGX, J. Appl. Crystallogr. 32 (1999) 837.
[40] L.J. Farrugia, J. Appl. Crystallogr. 30 (1997) 565.
[41] M.W. Schmidt, K.K. Baldridge, J.A. Boatz, S.T. Elbert, M.S. Gordon, J.H. Jensen, S. Koseki, N. Matsunaga, K.A. Nguyen, S. Su, T.L. Windus, M. Dupuis, J.A. Montgomery, J. Comput. Chem. 14 (1993) 1347–1363.